Available online at www.sciencedirect.com

ScienceDirect

www.elsevier.com/locate/matchar

The effect of spatial micro-CT image resolution and surface complexity on the morphological 3D analysis of open porous structures

Grzegorz Pyka[a,*], Greet Kerckhofs[a,b], Jan Schrooten[a], Martine Wevers[a]

[a]Department of Metallurgy and Materials Engineering, KU Leuven, Kasteelpark Arenberg 44 – PB2450, B-3001 Leuven, Belgium
[b]Biomechanics Research Unit, Université de Liege, Chemin des Chevreuils 1 - BAT 52/3, B-4000 Liège, Belgium

ARTICLE DATA

Article history:
Received 29 April 2013
Received in revised form
1 November 2013
Accepted 18 November 2013

Keywords:
3D morphological analysis
Micro computed tomography
Spatial resolution
Selective laser melting
Porous structures
Surface roughness

ABSTRACT

In material science microfocus X-ray computed tomography (micro-CT) is one of the most popular non-destructive techniques to visualise and quantify the internal structure of materials in 3D. Despite constant system improvements, state-of-the-art micro-CT images can still hold several artefacts typical for X-ray CT imaging that hinder further image-based processing, structural and quantitative analysis. For example spatial resolution is crucial for an appropriate characterisation as the voxel size essentially influences the partial volume effect. However, defining the adequate image resolution is not a trivial aspect and understanding the correlation between scan parameters like voxel size and the structural properties is crucial for comprehensive material characterisation using micro-CT. Therefore, the objective of this study was to evaluate the influence of the spatial image resolution on the micro-CT based morphological analysis of three-dimensional (3D) open porous structures with a high surface complexity. In particular the correlation between the local surface properties and the accuracy of the micro-CT-based macro-morphology of 3D open porous Ti6Al4V structures produced by selective laser melting (SLM) was targeted and revealed for rough surfaces a strong dependence of the resulting structure characteristics on the scan resolution. Reducing the surface complexity by chemical etching decreased the sensitivity of the overall morphological analysis to the spatial image resolution and increased the detection limit. This study showed that scan settings and image processing parameters need to be customized to the material properties, morphological parameters under investigation and the desired final characteristics (in relation to the intended functional use). Customization of the scan resolution can increase the reliability of the micro-CT based analysis and at the same time reduce its operating costs.

1. Introduction

Since two decades, microfocus X-ray computed tomography (micro-CT) is one of the reference techniques for non-destructive and three-dimensional (3D) visualisation and quantification of the internal structures of materials [1–3]. The popularity of micro-CT is growing rapidly together with a constant development of X-ray tubes and detectors which significantly increase the attainable spatial resolution down to sub-micron and nano-level [4] and at the same time extend the range of

* *Corresponding author at:* Department of Metallurgy and Materials Engineering, Katholieke Universiteit Leuven, Kasteelpark Arenberg 44 – PB2450, 3001 Leuven, Belgium. Tel.: +32 16 321194, +32 16 321300; fax: +32 16 321990.
E-mail address: gregory.pyka@mtm.kuleuven.be (G. Pyka).

1044-5803/$ – see front matter © 2013 Elsevier Inc. All rights reserved.
http://dx.doi.org/10.1016/j.matchar.2013.11.004

materials that can be examined. Therefore micro-CT is commonly used for morphological analysis of materials in many applications: biomedical [5,6], food science [7], materials science [8,9] as well as input for modelling [10] and for the optimisation of the production processes of complex structures using additive manufacturing (AM) techniques [11].

Despite constant system improvements, the images acquired using modern micro-CT devices can still hold several artefacts typical for tomographic imaging [12]. These are related to the stochastic properties of the X-ray radiation and its interactions with the object and detector. For example with polychromatic X-rays, the scatter and limited X-ray flux can be artefact sources in the reconstructed images hindering accurate structural analysis. Additionally, the spatial resolution is crucial for appropriate characterisation as the voxel size essentially influences the partial volume effect (PVE). The impact of both scan magnification and spatial image resolution on the qualitative analysis has been studied frequently [13–20]. For example, Cooper et al. [13] analysed the morphology of cortical bone using micro-CT images with varying voxel size, as appropriate quantification of the bone morphological properties is crucial for strength analysis and understanding the nature of the bone remodelling process. They demonstrated that the scan resolution significantly influenced the quantitative analysis of the bone structural parameters. Similar results were obtained by Peyrin et al. [16] and Kim et al. [17] as they observed that the mean trabeculae thickness analysed by micro-CT increased with increasing the voxel size. In materials science applications, Peng et al. [20] observed that a reduced spatial resolution resulted in an overestimated pore size and connectivity of Berea sandstone. For the morphological analysis of additive manufactured titanium alloy based porous structures Van Bael et al. [11] showed that the spatial resolution can limit the detectability of the smallest surface variations. Furthermore, Kerckhofs et al. [21] indicated that micro-CT based surface texture analysis of objects with different surface roughness depends on the image noise level and the surface complexity, as well as on the spatial image resolution. This implies that the morphological analysis of 3D porous structures with a complex surface morphology is strongly influenced by the voxel size of the reconstructed images. Therefore, methodologies that support optimal parameter selection are required.

Defining the adequate image resolution is not a trivial aspect and understanding the correlation between scan parameters like voxel size and the structural properties is crucial for comprehensive materials characterisation using micro-CT. Additionally, customizing the scan resolution to the material properties and morphological parameters under investigation can increase the reliability of the micro-CT based analysis and reduce its operating costs. Another important aspect is the compromise between the accuracy and the sample representativeness. Therefore, the objective of this study was to characterize the influence of the spatial image resolution as well as the surface complexity on the micro-CT-based morphological analysis of selective laser melting (SLM) produced 3D Ti6Al4V alloy based open porous structures with complex surface properties.

2. Materials and Method

2.1. *Ti6Al4V Open Porous Structures by SLM*

Cylindrical 3D open porous Ti6Al4V structures with a designed height and diameter of 6 mm (Fig. 1a), beam diameters of 100 and 180 μm respectively (Fig. 1b and c) and 1 mm pores were produced by SLM (Concept Laser GmbH, Germany). Four different structures were investigated in this study with respect to the designed beam thickness and the post-production surface treatment: i) as-produced structures with a designed beam thickness of 100 μm (further referred to as s.100ap), ii) as-produced structures with a designed beam thickness of 180 μm (further referred to as s.180ap), iii) surface treated structures with a designed beam thickness of 100 μm (further referred to as s.100CHE) and iv) surface treated structures with a designed beam thickness of 180 μm (further referred to as s.180CHE).

As reported by Pyka et al. [22] and shown in Fig. 1d and e, the SLM as-produced porous structures still contained a large amount of Ti6Al4V powder particles attached to the beam surface. The amount of necked powder particles increased with increasing beam diameter (Fig. 1d and e) and were mainly observed at the bottom (B) side of the beam in comparison to the top (T). These 3D porous structures with a high surface complexity were used to assess the effect of the voxel size on their morphological analysis by comparing the two beam diameters.

The 3D Ti6Al4V open porous structures consisted of several layers of thin beams/struts (Fig. 1d and e) at an angle of 45° to the building direction (Z axis in Fig. 1a, b, c and f) and were connected in the nodes (Fig. 1f). At the top and bottom of the structures, additional connecting beams were added to maintain the structure's integrity. Therefore, a full 3D structure consisted in the Z direction of three main sections with a significantly different local design: (i) 'base section' — present at the top and bottom of the structure, (ii) 'beam section' — with parallel arranged beams, and (iii) 'node section' — where the four beams are connected. Fig. 1g, h and i present typical micro-CT cross-sectional images of each section of a 3D Ti6Al4V open porous structure with a designed beam thickness of 180 μm. More information about the porous structure design and production can be found in Van Bael et al. [11].

2.2. *Surface Treatment of SLM Produced Ti6Al4V Open Porous Structures*

After SLM production, the 3D Ti6Al4V open porous structures were cleaned for 10 min in an ultrasonic bath in demineralised water, flushed with ethanol and air-dried to remove loose surface impurities and remaining loose powder particles from the pores. Next chemical etching (CHE) was performed by immersing the samples in a chemical solution based on hydrofluoric acid (HF) to dissolve the attached powder particles according to the protocol described by Pyka et al. [22]. After CHE, the porous structures were rinsed with demineralised water, then rinsed with ethanol and finally air-dried.

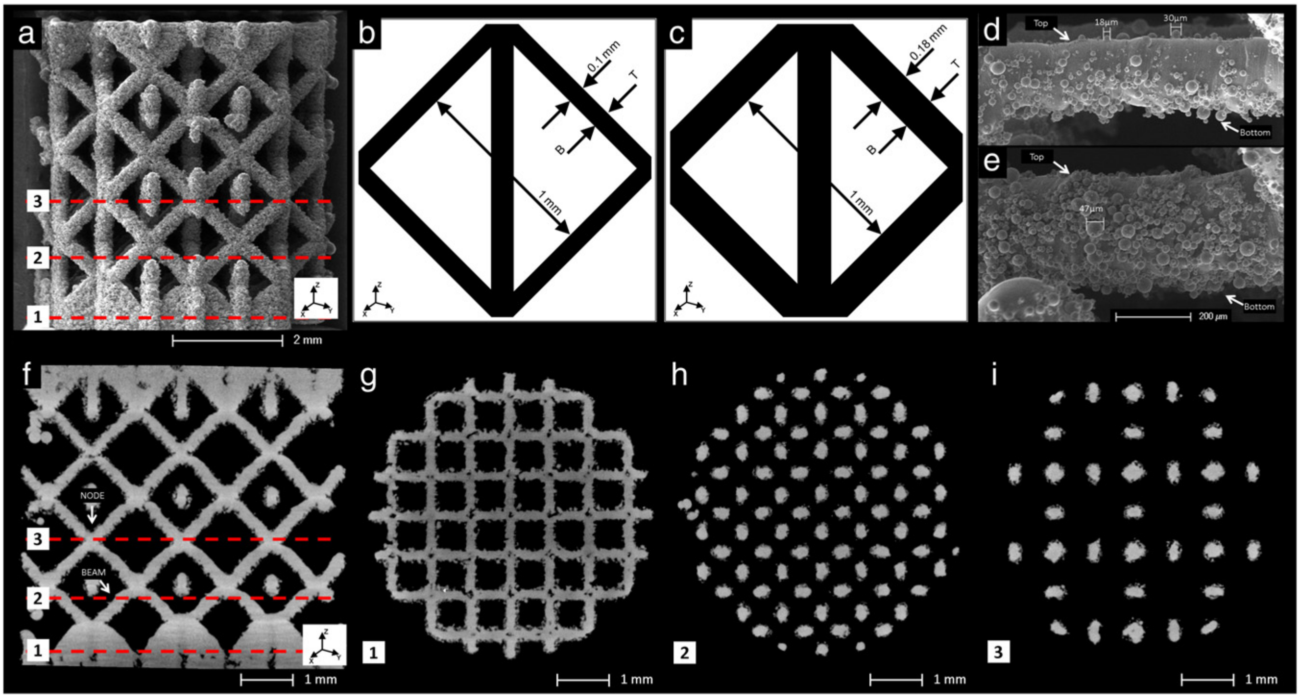

Fig. 1 – (a) Typical SEM micrograph of a 3D Ti6Al4V open porous structure, cross-section of the STL design of a single unit cell of a 3D Ti6Al4V open porous structure with designed beam size (b) 100 μm and (c) 180 μm, SEM micrographs of a single beam of a 3D Ti6Al4V open porous structure produced with designed beam size (d) 100 μm and (e) 180 μm. Typical micro-CT images of a 3D Ti6Al4V open porous structure with designed beam size 180 μm at a voxel size of 6.5 μm: cross section (f) along the building direction, (g) at the bottom, (h) in the middle highlighting the beams and (i) in the middle highlighting the nodes. The "Z" axis (a–f) shows the building direction. The top (T) and bottom (B) sides of the beams are indicated in b–e.

2.3. *Morphological Characterisation*

2.3.1. *Macro-level Morphological Characterisation*

Micro-CT based morphological characterisation of the 3D Ti6Al4V open porous structures, prior to (s.100a-p and s.180a-p) and after surface treatment (s.100CHE and s.180CHE), was performed by using a Phoenix NanoTom S (GE Measurement and Control Solutions, Germany) with a 180 kV/15 W high-performance nanofocus X-ray tube and a 2304 × 2304 pixel Hamamatsu detector. The device was equipped with a tungsten target and the applied voltage and current were 90 kV and 240 μA, respectively. A 0.3 mm copper filter was used. The exposure time was 500 ms and a frame averaging of 1 and image skip of 0 were applied resulting in a total sample scan time of 20 min. The tested samples were examined with two isotropic voxel sizes, namely 6.5 μm (high resolution) and 12.6 μm (low resolution). After scanning, the radiographs were reconstructed using Phoenix datos|x 2.0 reconstruction software. An automatic single-level 3D Otsu segmentation algorithm was applied for binarization of the reconstructed micro-CT images [23]. Additionally, to evaluate the influence of the segmentation method on the morphological analysis, a two- and three-level 3D Otsu segmentation algorithm were applied to binarize images of the structures s.180ap. CTAn software (Bruker micro-CT, Kontich, Belgium) was applied for the 3D morphological analysis of the micro-CT data. The total porosity (Po(tot)), closed porosity (Po(cl)), structure thickness (St.Th), beam thickness (B.Th) and object surface area (Obj.S) were calculated for the as-produced and surface treated samples.

As a reference, the pore volume fraction of the porous Ti6Al4V structures was determined using the Archimedes' principle using a Sartorious YDK 01, YDK 01-0D Density Determination Kit, following Method1. The density of an immersed object relative to the density of the fluid was calculated Eq. (1), in which all variables are measured in the laboratory except for the density of the sample, which is the only unknown. The porosity is then measured by multiplying the density of the sample by the sample volume (as measured using a caliper).

$$\frac{\textit{Sample density}}{\textit{Fluid density}} = \frac{\textit{Sample weight}}{\textit{Sample weight–Sample apparent weight (immersed)}} \quad (1)$$

The structure thickness was calculated in 3D using a sphere-fitting algorithm [24] and was visualised with a colour representation. The beam thickness was defined as the maximum of the structure thickness distribution.

2.3.2. *Surface Roughness Characterisation*

Visual observation of a single beam was done by scanning electron microscopy (SEM - Philips XL30 FEG, Germany). The quantification of the beam surface roughness (S.Rs) was performed by a micro-CT based protocol described by Kerckhofs et al. [20]. In brief, the profile lines of the beam surface extracted from the 2D cross-sectional images were used to calculate the arithmetic mean deviation of the roughness profile (P_a) (in correspondence with ISO 4287–1997 [25], but not taking into account the proposed measuring length since in 3D porous materials, the proposed measuring length was not available). To assess the influence of the spatial image resolution the difference in powder grain attachment to the bottom (B) and top (T) part of the beams was used. The beam surface roughness at the top and bottom was quantified prior to and after surface treatment.

2.4. *Statistical Analysis*

A 1-way ANOVA test was performed to analyse batch variations using Analyse-it version 2.25. For all results, p-values were determined and considered not significant when larger than 0.05. For all parameters the relative difference (d_r) was calculated using Eq. (2) to evaluate the errors in the results of morphological characterisation of the porous structures (i) scanned with different resolution and (ii) before and after surface treatment.

$$d_r = \frac{|x-y|}{\left(\frac{|x|+|y|}{2}\right)} * 100\,[\%] \tag{2}$$

with x and y corresponding to the chosen morphological parameter characteristic based on micro-CT images (i) obtained from scans with voxel sizes 6.5 and 12.6 μm respectively (analysis of the image resolution influence) and (ii) obtained for as-produced and surface treated structures respectively (analysis of the surface treatment effect).

3. Results

Qualitative evaluation (Fig. 2a and b) of the reconstructed images of structures s.180ap revealed a difference for the different segmentation methods. The structure in the binarized cross-sections using the two-level 3D Otsu was thicker compared to the single- and three-level 3D Otsu method. This resulted in a significantly lower porosity compared to the physically measured porosity (Fig. 3). For both the single- and three-level and 3D Otsu method no significant difference was observed with the Archimedes-based porosity measurement (Fig. 3). However, the single-level 3D Otsu method revealed a closer match to the Archimedes' results (0.4% of relative difference) in comparison to three-level 3D Otsu method (1.9% of relative difference) for data acquired with 6.5 μm voxel size. Typical detailed micro-CT 2D cross-sections of a single beam of a Ti6Al4V open porous structure, with a designed beam size of 180 μm scanned at 6.5 μm and 12.6 μm voxel size (Fig. 2a and b), show a clear impact of the voxel size on the detection limit of small structural details (i.e. particles attached to the beam surface). A voxel size of 6.5 μm showed to be more accurate to visualise these features, whereas the image quality at lower spatial resolution was inadequate to capture these structural details. After image segmentation, required for subsequent image analysis, the influence of the spatial resolution was even more clear (Fig. 2a and b).

Comparison of the total porosity calculated based on the Archimedes' principle and micro-CT image analysis using the single-level 3D Otsu segmentation method, showed a good correlation. No significant differences with the physical measurements were observed for all structures when scanned with voxel size 6.5 μm. For structures s.100ap, s.180ap and s.180CHE the significant difference in porosity was observed with the results from Archimedes and CT data with 12.6 μm voxel size (Fig. 4).

Quantitative structural analysis of the open porous structures revealed a significant dependency on the voxel size (Fig. 5). Almost all parameters analysed prior to and after surface treatment showed this voxel size dependency. The morphological parameters calculated for as-produced structures of both designs were significantly different as function of the scan resolution. Although the total porosity was the least influenced by the scan resolution, the porosity of the as-produced samples scanned with a voxel size of 6.5 μm was significantly higher in comparison to scans with a voxel size of 12.6 μm. After surface treatment, however, the porosity did not show any significant difference for both designs in function of the image resolution. The relative change of total porosity caused by CHE was low (about 5–6% for all designs regardless of the voxel size) as compared to other structural parameters. In contrast, the closed porosity was found to be the most sensitive to the image resolution used, resulting in relative differences for a different voxel size of 148% and 127% for structure s.100a-p and s.180a-p respectively. A smaller difference was noticed after surface treatment for structure s.180CHE (56.8%). Additionally, a reduction in closed porosity of about 50% was observed after CHE as indicated in the 6.5 μm scan results. Analysis of the average structure thickness also revealed a significant voxel size dependence, regardless of the structure design. The average structure thickness was higher when a low scan resolution was applied. Additionally, the relative difference after surface treatment was larger in the case of a 12.6 μm voxel size scan. A similar observation was found for the beam thickness, except for the s.100CHE condition, where no significant difference for the different voxel size scan results was found. The object surface presented a similar trend as the closed porosity, i.e. the results obtained from the higher resolution scans were significantly larger for both designs, also after surface treatment. However, in general a higher sensitivity to the voxel size was observed for as-produced samples compared to the surface treated samples. Additionally, for the s.100CHE structures a larger object surface reduction was found compared to the s.180CHE structures.

The surface roughness obtained by micro-CT image processing using two different resolutions provided two distinctly different beam surface morphology values. The P_a values derived from the 6.5 μm voxel size (high resolution) scans showed a significant difference between the roughness of the top and bottom of the beams, while for the low resolution (12.6 μm) the difference was not significant. Furthermore, for all conditions the roughness was higher when analysed using the high resolution images. Especially for the bottom part of the beams, a significant dependence of the P_a value on the voxel size was observed, expect for the s.100CHE structures.

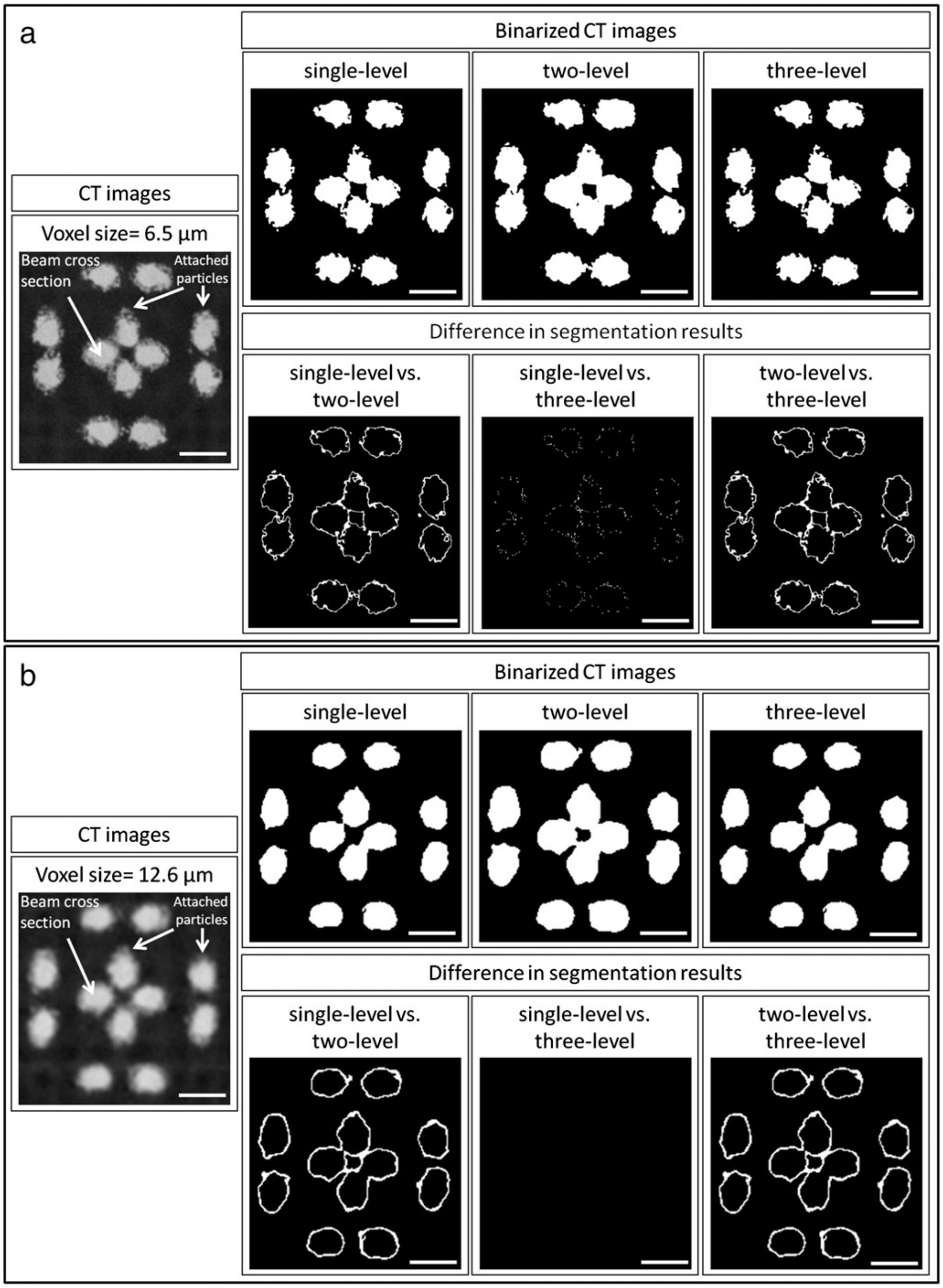

Fig. 2 – Typical grey-scale and binarized cross-sectional micro-CT images of the beams of as-produced Ti6Al4V porous structure manufactured with a designed beam thickness of 180 μm and scanned with voxel size of 6.5 μm. The segmentation was performed using different methods namely: Single-level, two-level and three-level 3D Otsu segmentation. Scale bars = 500 μm.

Fig. 6a and b shows the structure thickness distribution for the different voxel sizes both for as-produced and surface treated samples with a beam thickness of 100 μm and 180 μm respectively. For the low resolution scans, two distinct characteristic peaks are visible, representing the beam and node thickness respectivel y. When using the higher spatial resolution scans a third peak becomes visible that corresponds to the particles attached to the beam surface. The beam thickness visualisation by a sphere fitted colour representation on the analyzed structure (Fig. 7) shows for the high resolution scans that the particles attached to the beam surface were marked with a different colour compared to the beam cross section. As the voxel size increased, the particles were merged with the beam section and as a result larger spheres were fitted and no more particles could be observed at the beam surface. This sphere fitted analysis explains the presence of the third peak in the structure thickness distribution for the 6.5 μm voxel size (Fig. 6). Moreover, after

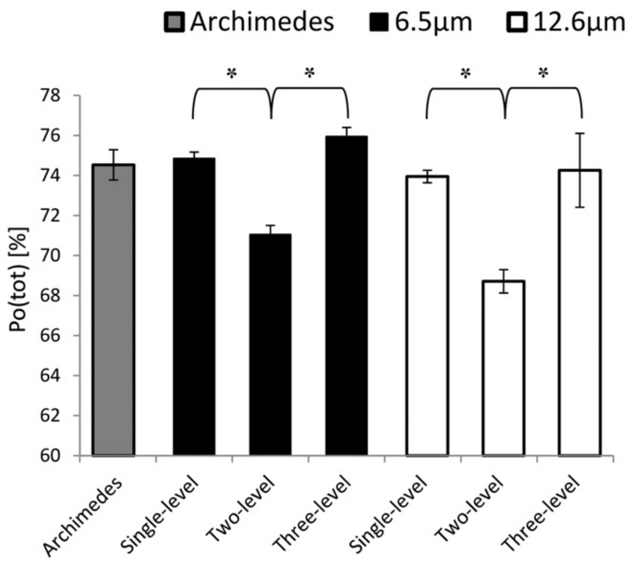

Fig. 3 – Comparison of the porosity calculated for the as-produced Ti6Al4V porous structures manufactured with a designed beam thickness of 180 μm based on the Archimedes' principle and via micro-CT analysis of the images acquired with a voxel size of 6.5 μm and 12.6 μm. The segmentation was performed using the single-level, two-level and three-level 3D Otsu method. (* $p < 0.05$ — significant difference).

surface treatment the structure thickness distribution showed a decrease of the third peak, which corresponds to the removal of particles by chemical etching.

4. Discussion

The objective of this study was to evaluate the influence of the voxel size on the micro-CT based morphological analysis of 3D open porous structures with a high surface complexity, with the specific goal to establish the influence of the local roughness on the accuracy of the micro-CT based macro-level morphology of the 3D porous structures. To ensure the availability of suitable structures, SLM was selected as it provides the possibility to produce 3D open porous structures with controlled overall morphological properties in a robust way, which was confirmed by a micro-CT based morphological quality control in Ref. [11]. However, it was concluded that the applied spatial resolution of 12.6 μm voxel size might be insufficient to detect the smallest, SLM related surface variations such as the attached powder particles. Indeed, as reported by Pyka et al. [22] and shown in this study (Fig. 1d and e) the powder particles attached to the beam surface of SLM porous structures introduced an average roughness deviation from the profile line (P_a) of about 12 μm. This implies that the voxel size should be smaller than 12.6 μm to capture these surface details by micro-CT based morphological analysis. Additionally, it was shown that measurement errors such as local and random surface deviations introduced by inaccurate CT setup parameters can affect precise analysis of the object dimensions [26]. However there is still little known on how the surface irregularities influence micro-CT based morphological characterization of complex porous structures. Although the influence of spatial image resolution on micro-CT based morphological analysis has been studied frequently [13–20], the influence of the local surface properties of 3D porous structures on the accuracy of the micro-CT based macro-structural analysis has not been defined yet.

In the case of micro-CT characterisation of SLM produced 3D open porous structures, the particles attached to the beam surface influence the PVE, which is one of the typical artefacts in micro-CT images [12], as shown by representative 2D cross-sectional images from 6.5 μm and 12.6 μm scans in Fig. 2a and b. The high resolution scan provided more detailed information about the beam surface morphology while in the low resolution scan the sharpness of the edges was progressively distorted. This resulted in less information about the

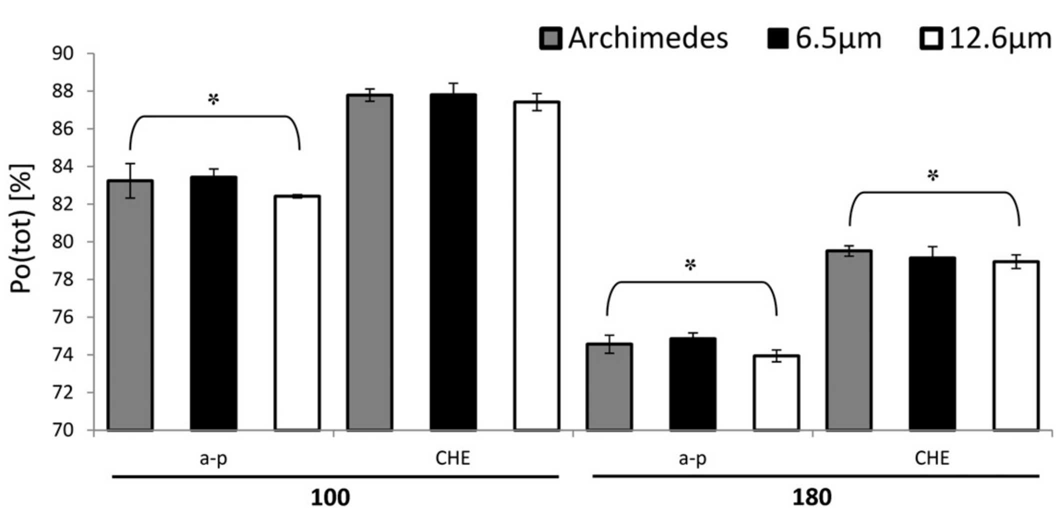

Fig. 4 – Comparison of the porosity calculated for the as-produced Ti6Al4V porous structures manufactured with a designed beam thickness of 100 μm and 180 μm based on the Archimedes' principle and via micro-CT analysis of the images acquired with a voxel size of 6.5 μm and 12.6 μm. The segmentation was performed using the single-level 3D Otsu method. (* $p < 0.05$ — significant difference).

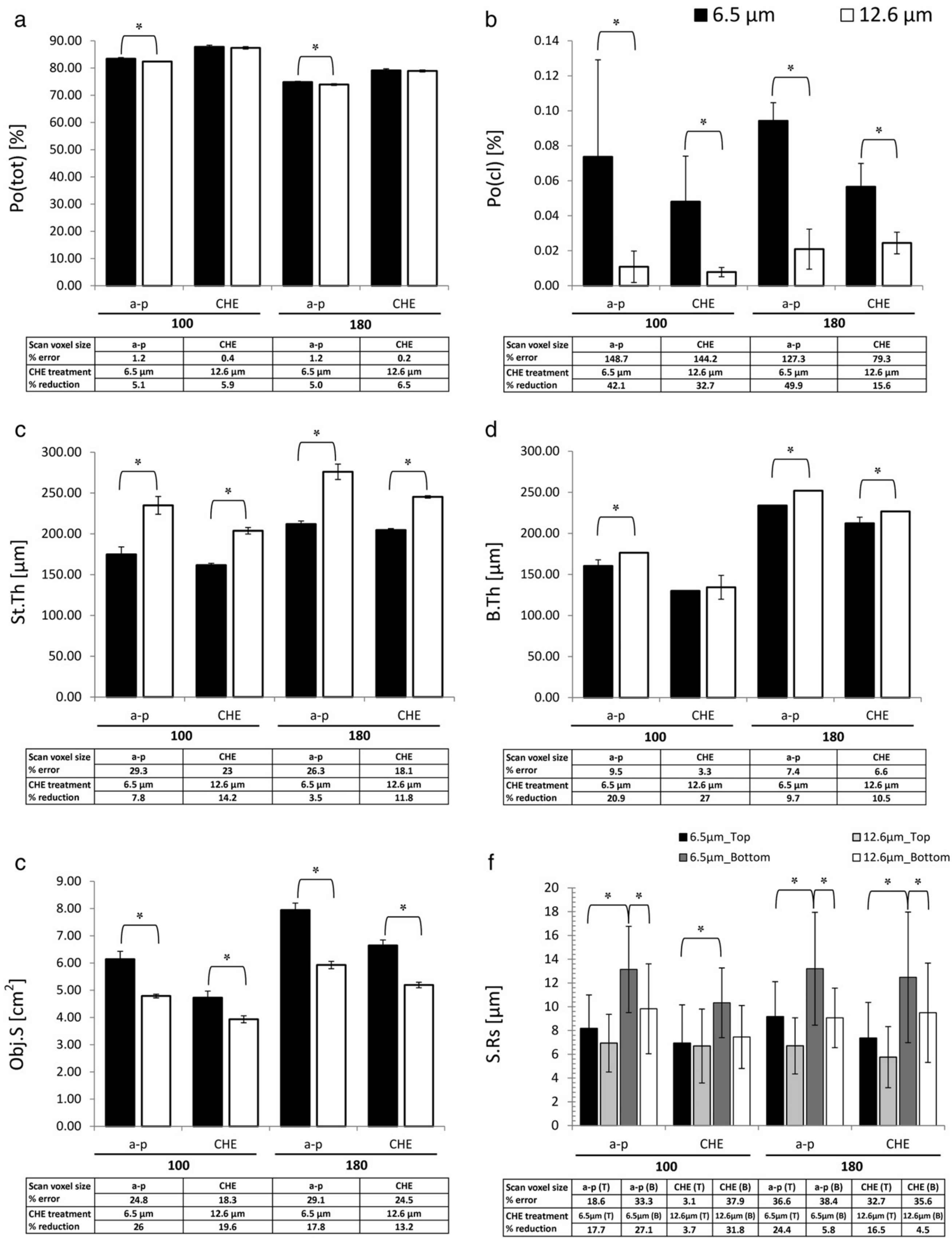

(a)

Scan voxel size	a-p	CHE	a-p	CHE
% error	1.2	0.4	1.2	0.2
CHE treatment	6.5 μm	12.6 μm	6.5 μm	12.6 μm
% reduction	5.1	5.9	5.0	6.5

(b)

Scan voxel size	a-p	CHE	a-p	CHE
% error	148.7	144.2	127.3	79.3
CHE treatment	6.5 μm	12.6 μm	6.5 μm	12.6 μm
% reduction	42.1	32.7	49.9	15.6

(c)

Scan voxel size	a-p	CHE	a-p	CHE
% error	29.3	23	26.3	18.1
CHE treatment	6.5 μm	12.6 μm	6.5 μm	12.6 μm
% reduction	7.8	14.2	3.5	11.8

(d)

Scan voxel size	a-p	CHE	a-p	CHE
% error	9.5	3.3	7.4	6.6
CHE treatment	6.5 μm	12.6 μm	6.5 μm	12.6 μm
% reduction	20.9	27	9.7	10.5

(e)

Scan voxel size	a-p	CHE	a-p	CHE
% error	24.8	18.3	29.1	24.5
CHE treatment	6.5 μm	12.6 μm	6.5 μm	12.6 μm
% reduction	26	19.6	17.8	13.2

(f)

Scan voxel size	a-p (T)	a-p (B)	CHE (T)	CHE (B)	a-p (T)	a-p (B)	CHE (T)	CHE (B)
% error	18.6	33.3	3.1	37.9	36.6	38.4	32.7	35.6
CHE treatment	6.5μm (T)	6.5μm (B)	12.6μm (T)	12.6μm (B)	6.5μm (T)	6.5μm (B)	12.6μm (T)	12.6μm (B)
% reduction	17.7	27.1	3.7	31.8	24.4	5.8	16.5	4.5

Fig. 5 – Macro-level morphological parameters of 3D Ti6Al4V open porous structures calculated from micro-CT images with a voxel size of 6.5 and 12.6 μm, for the as-produced and surface treated samples with a designed beam thickness of 100 and 180 μm: (a) total porosity (Po-Tot), (b) closed porosity (Po-Clo), (c) average structure thickness (Av-St.Th), (d) average beam thickness (Av-B.Th), (e) object surface area (Obj.S) and (f) beam surface roughness — Pa (S.Rs).

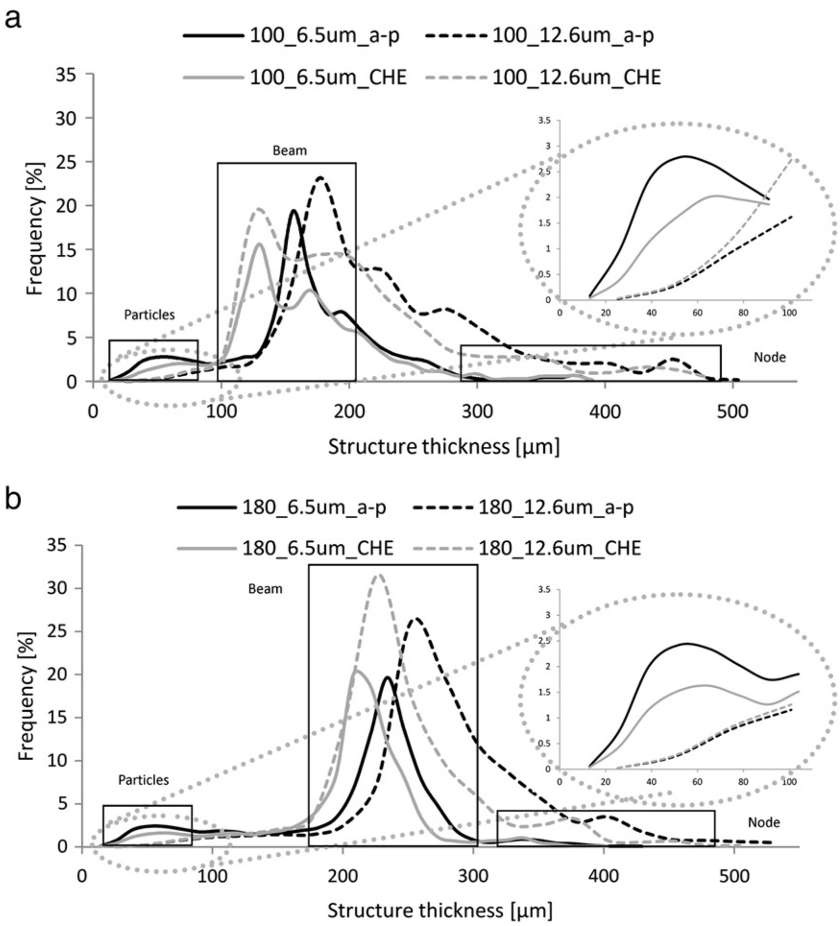

Fig. 6 – Structure thickness distribution of 3D Ti6Al4V open porous structures calculated from micro-CT images with a voxel size of 6.5 and 12.6 μm for the as-produced and surface treated samples with a designed beam thickness of (a) 100 μm and (b) 180 μm. The left peak in the distribution plots represents the particles, the middle peak the beams and the right peak the nodes in the 3D Ti6Al4V open porous structures.

local structural properties. Additionally, the PVE has an indirect effect on the image segmentation as discussed in Ref. [27] and shown in Fig. 2a and b. Because of a bimodal grey value distribution in the micro-CT images, and thus an overlapping of the intensity distributions of the material and the background, finding the optimal segmentation threshold was a critical step in the image analysis. An example of the influence of the segmentation method on the morphological analysis is shown in Fig. 2a and b. Additionally, the segmentation results can be influenced by the image spatial resolution [27]. Therefore, in this study a single-level automatic 3D Otsu segmentation algorithm [23] was applied, which is a user-independent and more reproducible method compared to manual segmentation, to define the most optimal threshold value. Although being automatic, this algorithm is not independent of the material, architecture type, image quality and spatial resolution, and thus the threshold value will change when one of these parameters change.

Many thresholding methods have been developed [23,28–32] and their impact on 3D microstructural analysis has been studied frequently [33–36]. Kastner et al. [32] determined an optimal segmentation approach for pore detection in fibre reinforced composites. They showed that the porosity measurements, by applying their thresholding algorithm, were independent of the voxel size. In our study the total porosity analysis was for all designs dependent on the scan resolution, however this dependence was only significant for as-produced samples with a high surface roughness and not after surface treatment. A lower porosity was observed when a lower image resolution was applied (Fig. 5a) as the attached powder particles enhanced the PVE. It is important to underline that the voids present in the composite materials investigated by Kastner et al. [32] had a smooth surface and that the material and pore phases could be easily distinguished. This condition corresponded well to the porosity analysis results of the surface treated structures in this study. Additionally, it was shown in this study that the single-level automatic 3D Otsu segmentation approach provides reliable data as the porosity analysis closely matched the reference results obtained based on the Archimedes' principle.

In the case of as-produced samples scanned at lower resolution, the attached particles seemed to be merged with the beam surface, which resulted in a larger average beam thickness (Fig. 5d) and thus a lower overall porosity. As a result of this resolution dependence and because the surface treatment removed attached particles, no significant difference in total porosity was observed for both designs, independent of the

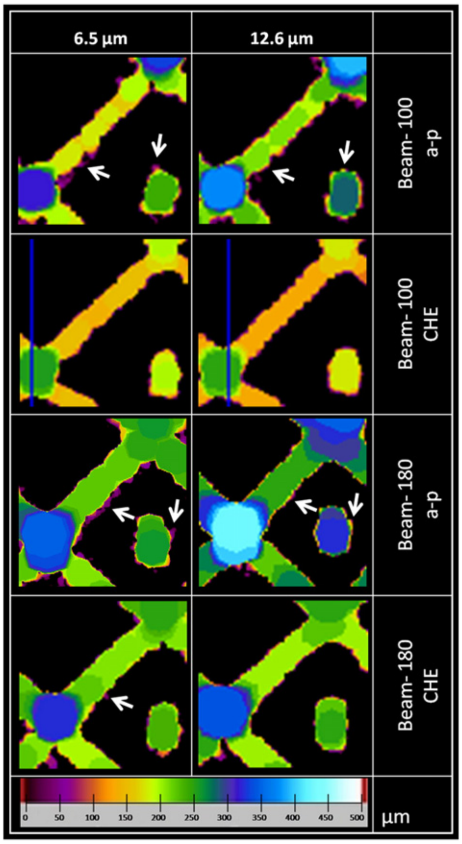

Fig. 7 – Visualisation of the sphere-fitting process applied to the micro-CT images for the calculation of the structure thickness distribution for 3D Ti6Al4V open porous structures with a designed beam thickness of 100 μm and 180 μm prior to and after surface treatment, both for images with a voxel size of 6.5 μm and 12.6 μm. Each colour corresponds to a different size of fitted spheres. White arrows indicate the powder particles attached to the surface.

voxel size. Additionally, in the binary images at a voxel size of 6.5 μm the attached powder particles were visible and also small pores enclosed by these particles could be observed. This resulted in a higher closed porosity calculated from the 6.5 μm compared to the 12.6 μm scans as presented in Fig. 5b. Similar findings were reported in another study [20] showing that low resolution micro-CT can still capture the large-pore porosity in the Berea sandstone. However, it was noticed that a low resolution scan underestimates the small-pore porosity and pore connectivity. In the case of 3D porous structures investigated in this study, reduction in closed porosity, introduced by the surface treatment, of about 40% and 50% for structures with a designed beam thickness of 100 and 180 μm respectively, confirmed that the closed porosity was indeed mainly a result of the powder particles attached to the beam surface.

The 12.6 μm scans resulted in a larger beam diameter, which also influenced the St.Th and B.Th values as both parameters were significantly larger for the 12.6 μm voxel size scans. Similar findings were observed in Refs. [13–17] for the analysis of the mean cortical and trabecular bone thickness in function of the voxel size. According to Cooper et al. [13], the difference was caused by a loss of detection of smaller trabeculae when the voxel size increased, which resulted in a larger mean thickness. In our study we can see that the measurements of the beam thickness based on micro-CT images with a different resolution were influenced by the surface complexity as in the low resolution scan the attached particles were merged with the beam, which resulted in larger mean beam size.

As for 3D open porous structures it is shown for the micro-CT based morphological analysis that the local surface properties are influenced by the spatial image resolution used, one has to take care of further usage of the resulting morphological values for functional material property analyses, such as fluid dynamics [37,38], optical properties [39], frictional behaviour [40], heat transfer [41] and mechanical properties [42]. As presented in Fig. 5e the surface area analysis of 3D Ti6Al4V open porous structures strongly depends on the scan voxel size. The surface area calculated based on the high resolution scans resulted in higher values than those from low resolution scans. This corresponds to findings reported in Refs. [43,44]. However in our study this effect was exemplified by the fact that more surface details were captured in the high resolution scan, which also resulted in a larger total surface area. Since the surface treatment etched away material and removed particles from the beam surface, the surface area decreased. Additionally the decrease in surface area by the surface treatment was smaller for structures with a designed beam thickness of 180 μm compared to the ones with 100 μm designed beam thickness, which could be related to the limited efficacy of the used surface treatment conditions for the latter design. This implies that the combination of an appropriate treatment with an accurate morphological analysis is crucial for controlled post-production surface roughness modification of 3D porous structures produced by SLM.

Quantitative surface roughness analysis of 3D Ti6Al4V porous structures is more complex than an overall morphological characterization. The relatively high surface roughness, small beam diameter and 5D outer and internal architecture of these structures do not allow the use of standard profile measurement systems, like atomic force microscope or optical profilometry. Therefore high resolution micro-CT was applied for the quantitative surface roughness measurements, as described in Kerckhofs et al. [21]. Only the high resolution scans revealed a significant difference in P_a value between these two beam sections. The low resolution scans were insufficient to capture correctly the beam surface variations. This corresponded to the results obtained by Kerckhofs et al. [21], where it was shown that the roughness of 2D SLM-produced Ti6Al4V plates with a complex surface depended on the spatial resolution and surface complexity. In the case of SLM-produced 3D structures the surface roughness by the attached particles influences the required image resolution for accurate 3D morphological analysis.

Defining the appropriate image resolution for micro-CT based material characterisation is not trivial as it requires a proper understanding of the correlation between scan parameters like voxel size and the structural material properties under investigation. This study shows the need for matching micro-CT device settings with the material under investigation to generate reliable morphological data for further material analysis. However, often the selection of scan parameters must compromise between the accuracy and the sample representativeness as increasing the scan resolution reduces the sample volume that can be investigated. This is crucial especially for the characterization of complex porous materials with an inhomogeneous structure and pore size distribution. Additionally, the economical and/or safety aspects can limit micro-CT based analysis. For instance a higher resolution or frame averaging results in a better image quality as the signal-to-noise ratio and sharpness increases. However, this can only be accomplished with longer scanning time thus higher running costs and higher radiation dose [45]. Furthermore, the spatial image resolution significantly influences the subsequent image processing and analysis time as well as disc space required for data storage due to the image file size. Therefore, customization of the voxel size to the research objectives/parameters of choice can significantly reduce the cost of the micro-CT analysis while maintaining the required minimal setting to obtain suitable images, which can become an issue especially in the case of large-scale, routine experiments and/or quality assessments.

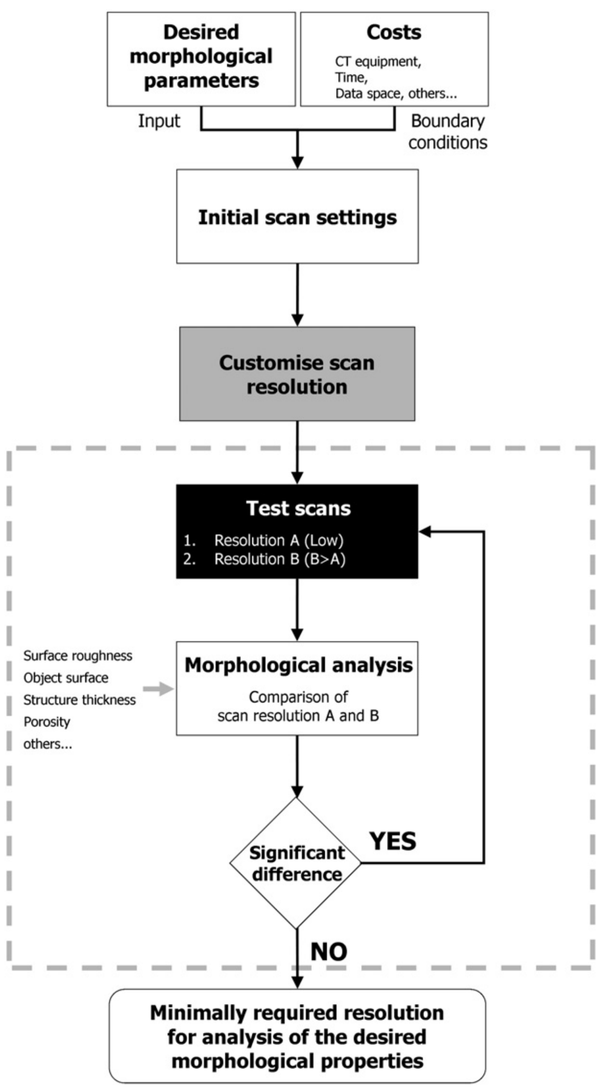

Fig. 8 – Process algorithm for customisation of the scan resolution to the morphological material properties under investigation.

Fig. 8 proposes an iterative algorithm that customises the scan resolution to the morphological material properties under investigation, taking into account the practical limitations of the micro-CT device at hand. The procedure for scan resolution optimisation finds the minimal image resolution by reducing the image voxel size until there is no significant difference for the desired morphological properties between two consecutive scans. For instance, as presented in Fig. 5a and d, no significant difference between scans with voxel size of 6.5 μm and 12.6 μm was observed for the analysis of the porosity of both surface modified structure designs and for the beam thickness of structure s.100CHE. Thus, for the analysis of those parameters the low resolution scan (12.6 μm) would be sufficient and one can save on image storage capacity and processing time.

In contrast, the surface area and roughness were still significantly different for both scan resolutions (6.5 μm and 12.6 μm), indicating that the surface complexity of as-produced and surface treated structures was still too high to be captured with the low resolution scan (12.6 μm). Similar findings were reported in other studies [45,46]. It was shown that an increased voxel size within a test range did not result in a higher accuracy of the 3D surface models of mandibles [45]. Tkachenko et al. [46] defined the resolution threshold below in which an increase in voxel size of micro-CT images did not affect anymore the identification of the resorption cavities in bone surface morphology. Furthermore, Peng et al. [20] concluded that for rock samples the resolution for permeability analysis could be lower than that for diffusion analysis. This implies that there is no unique scan resolution optimal for analysis of a wide range of morphological parameters. This study confirmed that for an accurate analysis of different morphological parameters of 3D porous structures different resolutions might be required. Thus, to obtain an optimal balance between the scan cost and the quality of micro-CT based analysis the scan resolution should be fine-tuned according to the morphological parameters under investigation.

5. Conclusions

This study investigated for the morphological characterization of complex 3D Ti6Al4V open porous structures the effect of the spatial micro-CT image resolution and showed a relation between the voxel size used, the specific surface complexity of the material under investigation and the reliability of the resulting morphological properties. As the PVE was enhanced by the surface complexity, and it was more pronounced in the low resolution images, the detection of morphological surface details required a higher resolution. As the surface treatment reduced the surface roughness, the beams and nodes remained the smallest structural features that could be resolved by micro-CT analysis. Due to this reduced surface complexity, a lower spatial image resolution was sufficient to capture the relevant morphological properties. From all morphological parameters under investigation, the total porosity was the least sensitive to the surface complexity and scan voxel size. On the other hand, local morphological properties like surface roughness, surface area and closed porosity showed the strongest dependency on the voxel size, as these properties were more directly related to the high surface complexity of the 3D open porous structures. Also the average structure and beam thickness depended on the spatial resolution of the micro-CT images and the local surface morphology.

To conclude, it is critical for micro-CT characterization to find a proper trade-off between the desired image quality, in relation to the (functional) material properties under investigation, on the one hand and the scan time and image processing on the other hand. Hence the above-mentioned findings can assist to increase the quality of 3D quantitative morphological analysis of any object in relation to its surface complexity as well as to reduce the investigation time and costs by evolving towards a customised relationship of micro-CT setting versus morphological analysis level.

Acknowledgement

Grzegorz Pyka was funded by the Research Foundation, Flanders (FWO, G.0618.10). Greet Kerckhofs was funded by the Agency for Innovation by Science and Technology in Flanders (IWT/OZM/090655) and acknowledges the European Research Council under the European Union's Seventh Framework Program (FP7/2007-2013)/ERC grant agreement no. 279100. The authors would like to acknowledge the Hercules foundation for funding the project AKUL/09/001 "Micro- and nano-CT for the hierarchical analysis of materials" and the IAP project P7/21 INTEMATE, "Multiscale mechanics of INTErface dominated MATErials", for the financial support.

REFERENCES

[1] Landis EN, Keane DT. X-ray microtomography. Mater Charact 2010;61:1305–16.
[2] Bonse U. X-Ray imaging: past and present. Proc SPIE 2008;7078:707802.
[3] Elliott JC, Davis GR, Dover SD. X-ray microtomography, past and present. Proc SPIE 2008;7078:707803.
[4] Dierick M, Van Hoorebeke L, Jacobs P, Masschaele B, Vlassenbroeck J, Cnudde V, et al. The use of 2D pixel detectors in micro- and nano-CT applications. Nucl Instrum Methods A 2008;591:255–9.
[5] Mitzutani R, Suzuki Y. X-ray microtomography in biology. Micron 2012;43:104–15.
[6] Tjong W, Kazakia GJ, Burghardt AJ, Majumdar S. The effect of voxel size on high-resolution peripheral computed tomography measurements of trabecular and cortical bone microstructure. Med Phys 2011;39:1893–903.
[7] Pareyt B, Talhaoui F, Kerckhofs G, Brijs K, Goesaert H, Wevers M, et al. The role of sugar and fat in sugar-snap cookies: structural and textural properties. J Food Eng 2009;90(3):400–8.
[8] Baker DR, Mancini L, Polacci M, Higgins MD, Gualda GAR, Hill RJ, et al. An introduction to the application of X-ray microtomography to the three-dimensional study of igneous rocks. Lithos 2012;148:262–76.
[9] Herrero JM, Germain Ch. Microstructure reconstruction of fibrous C/C composites from X-ray microtomography. Carbon 2007;6:1242–53.
[10] Truscello S, Kerckhofs G, Van Bael S, Pyka G, Schrooten J, Van Oosterwyck H. Prediction of permeability of regular scaffolds for skeletal tissue engineering: a combined computational and experimental study. Acta Biomater 2012;8:1648–58.
[11] Van Bael S, Kerckhofs G, Moesen M, Pyka G, Schrooten J, Kruth JP. Micro-CT-based improvement of geometrical and mechanical controllability of selective laser melted Ti6Al4V porous structures. Mater Sci Eng A 2011;528:7423–31.
[12] Vincken KL, Koster AE, Viergever MA. Probabilistic segmentation of partial volume voxels. Pattern Recogn Lett 1994;15:477–84.
[13] Cooper D, Turinsky A, Sensen C, Hallgrimsson B. Effect of voxel size on 3D micro-CT analysis of cortical bone porosity. Calcif Tissue Int 2007;80:211–9.
[14] Müller R, Koller B, Hildebrand T, Laib A, Gianolini S, Rüegsegger P. Resolution dependency of microstructural properties of cancellous bone based on three-dimensional μ-tomography. Technol Health Care 1996;4:113–9.
[15] Kothari M, Keaveny TM, Lin JC, Newitt D, Genant H, Majumdar S. Impact of spatial resolution on the prediction of trabecular architecture parameters. Bone 1998;22:437–43.
[16] Peyrin F, Salome M, Cloetens P, Laval-Jeantet AM, Ritman E, Ruegsegger P. Micro-CT examinations of trabecular bone samples at different resolutions: 14, 7 and 2 micron level. Technol Health Care 1998;6(5–6):391–401.
[17] Kim DG, Christopherson GT, Dong XN, Fyhrie DP, Yeni YN. The effect of microcomputed tomography scanning and reconstruction voxel size on the accuracy of stereological measurements in human cancellous bone. Bone 2004;35:1375–82.
[18] Langheinrich AC, Kampschulte M, Crössmann C, Moritz R, Rau WS, Bohle RM, et al. Role of computed tomography voxel size in detection and discrimination of calcium and iron deposits in atherosclerotic human coronary artery specimens. J Comput Assist Tomogr 2009;33(4):517–22.
[19] Moritz R, Eaker DR, Langheinrich AC, Jorgensen SM, Bohle RM, Ritman EL. Quantification of vasa vasorum density in multi-slice computed tomographic coronary angiograms: role of computed tomographic image voxel size. J Comput Assist Tomogr 2010;34(2):273–8.
[20] Peng S, Hu Q, Dultz S, Zhang M. Using X-ray computed tomography in pore structure characterization for a Berea sandstone: resolution effect. J Hydrol 2012;472 473:254–61.
[21] Kerckhofs G, Pyka G, Moesen M, Van Bael S, Schrooten J, Wevers M. High-resolution micro-CT as a tool for 3D surface roughness measurement of additive manufactured porous materials. Adv Eng Mater 2012. http://dx.doi.org/10.1002/adem.
[22] Pyka G, Burakowski A, Kerckhofs G, Moesen M, Van Bael S, Schrooten J, et al. Surface modification of Ti6Al4V open porous structures produced by additive manufacturing. Adv Eng Mater 2012;14:363–70.
[23] Otsu N. Threshold selection method from gray-level histograms. IEEE Trans Syst Man Cybern 1979;9(1):62–6.
[24] CTAn UserManual. http://www.skyscan.be/next/CTan_UserManual.pdf.
[25] ISO 4287. Geometrical Product Specifications (GPS) — Surface texture: Profile method — Terms, definitions and surface texture parameters; 1997.
[26] Nardelli V, Arenhart F, Donatelli G, Porath M, Niggemann C, Schmitt R. Feature-based analysis for quality assessment of x-ray computed tomography measurements. Meas Sci Technol 2012;23. http://dx.doi.org/10.1088/0957-0233/23/10/105006.
[27] Elmoutaouakkil A, Peyrin F, Elkafi J, Laval-Jeantet A. Segmentation of cancellous bone from high resolution

computed tomography images: influence on trabecular bone measurements. IEEE Trans Med Imaging 2002;21(4):354–62.
[28] Ding M, Odgaard A, Hvid I. Accuracy of cancellous bone volume fraction measured by micro-CT scanning. J Biomech 1999;32(3):323–6.
[29] Oh W, Lindquist WB. Image thresholding by indicator kriging. IEEE Trans Pattern Anal Mach Intell 1999;21(7):590–602.
[30] Waarsing JH, Day JS, Weinans H. An improved segmentation method for in vivo microCT imaging. J Bone Miner Res 2004;19(10):1640–50.
[31] Sheppard AP, Sok RM, Averdunk H. Techniques for image enhancement and segmentation of tomographic images of porous materials. Phys A 2004;339(1–2):145–51.
[32] Kastner J, Plank B, Salaberger D, Sekelja J. Defect and porosity determination of fibre reinforced polymers by X-ray computed tomography. 2nd International Symposium on NDT in Aerospace 2010 - We.1.A.2; 2010.
[33] Weszka JS. Survey of threshold selection techniques. Comput Vision Graph 1978;7(2):259–65.
[34] Sezgin M, Sankur B. Survey over image thresholding techniques and quantitative performance evaluation. J Electron Imaging 2004;13(1):146–68.
[35] Pal NR, Pal SK. A review on image segmentation techniques. Pattern Recogn 1993;26(9):1277–94.
[36] Rajagopalan S, Lu L, Yaszemski MJ, Robb RA. Optimal segmentation of microcomputed tomographic images of porous tissue-engineering scaffolds. J Biomed Mater Res A 2005;75A(4):877–87.
[37] Rostamy N, Bergstrom DJ, Sumner D, Bugg JD. The effect of surface roughness on the turbulence structure of a plane wall jet. Phys Fluids 2011;23:085103.
[38] Tian ZF, Inthavong K, Tu JY, Yeoh GH. Numerical investigation into the effects of wall roughness on a gas–particle flow in a 90° bend. Int J Heat Mass Transf 2008;51:1238–50.
[39] Zeman M, Van Swaau RACMM, Zuiddam M, Metselaar JW, Schropp REI. Effect of interface roughness on light scattering and optical properties of a-Si:H solar cells. MRS Proc 1999;557. http://dx.doi.org/10.1557/PROC-557-725.
[40] Leu DK. Modeling of surface roughness effect on dry contact friction in metal forming. Int J Adv Manuf Technol 2011;57(5–8):575–84.
[41] Yang L, Jing C, WeiZhong L, Ning Z. Effect of surface microstructure on microchannel heat transfer performance. J Heat Transf 2011;133(12):124501.
[42] Kotousov A, Neto LB, Rahman SS. Theoretical model for roughness induced opening of cracks subjected to compression and shear loading. Int J Fract 2011;172:9–18.
[43] Cooper D, Matyas J, Katzenberg M, Hallgrimsson B. Comparison of microcomputed tomographic and microradiographic measurements of cortical bone porosity. Calcif Tissue Int 2004;74:437–47.
[44] Muller R, Koller B, Hildebrand T, Laib A, Gianolini S, Ruegsegger P. Resolution dependency of microstructural properties of cancellous bone based on threedimensional mu-tomography. Technol Health Care 1996;4:113–9.
[45] Damstra J, Fourie Z, Huddleston Slater J, Ren Y. Accuracy of linear measurements from cone-beam computed tomography-derived surface models of different voxel sizes. Am J Orthod Dentofacial Orthop 2010;137(1). http://dx.doi.org/10.1016/j.ajodo.2009.06.016.
[46] Tkachenko E, Slyfield C, Tomlinson R, Daggett J, Wilson D, Hernandez C. Voxel size and measures of individual resorption cavities in three-dimensional images of cancellous bone. Bone 2009;45(3):487–92.